

Toward More Realistic Mass Functions For Ultradense Dark Matter Halos

SAEED FAKHRY,¹ MARZIEH FARHANG,¹ AND ANTONINO DEL POPOLO^{2,3,4}

¹*Department of Physics, Shahid Beheshti University, Evin, Tehran 19839, Iran*

²*Dipartimento di Fisica e Astronomia, University of Catania, Viale Andrea Doria 6, 95125 Catania, Italy*

³*Institute of Astronomy, Russian Academy of Sciences, Pyatnitskaya str. 48, 119017 Moscow, Russia*

⁴*Institute of Astronomy and National Astronomical Observatory, Bulgarian Academy of Sciences, 72, Tsarigradsko Shose Blvd., 1784 Sofia, Bulgaria*

ABSTRACT

Ultradense dark matter halos (UDMHs) are high concentrations of dark matter which are assumed to have formed from amplified primordial perturbations, alongside the primordial black holes (PBHs). In this work we calculate the abundance of UDMHs and improve the previous works by elaborating on the formation process of these halos through including various physical and geometrical modifications in the analysis. In particular, we investigate the impact of angular momentum, dynamical friction and triaxial collapse on the predicted mass functions for UDMHs. We perform the calculations for four primordial power spectra with different amplified features that allow for (PBH and) UDMH formation in a wide mass range. We find that the abundance of UDMHs is prominently enhanced in the presence of these more realistic physical modifications. Comparison of the results with the current observational bounds on PBHs also implies that the UDMHs are expected to significantly outnumber PBHs in broad mass intervals, with the details depending on the primordial power spectrum.

Keywords: Dark Matter – Primordial Black Hole – Gravitational Collapse – Galactic Halos

1. INTRODUCTION

Primordial black holes (PBHs) are macroscopic candidates for dark matter. They are believed to form from small-scale, large-amplitude primordial density fluctuations during the early stages of the Universe (see, e.g., Villanueva-Domingo et al. 2021; Green & Kavanagh 2021; Carr & Kuhnel 2021; Korwar & Profumo 2023). PBHs can have significant gravitational interactions that affect various cosmological observables. They can act as gravitational lenses (Wang et al. 2021; Cai et al. 2023), potentially influence the formation of large-scale structures, and also contribute to temperature fluctuations in the cosmic microwave background (Silk 2000). PBHs have also been proposed to explain gravitational waves resulting from black hole mergers (Bird

et al. 2016; Sasaki et al. 2016) and act as initial seeds for the formation of supermassive black holes (Carr & Silk 2018).

The constraints on the abundance of PBHs heavily depend on the model for their mass distribution (Carr et al. 2021). Various studies suggest that PBH mergers within a narrow mass range during the late-time Universe could align with the detected gravitational waves arising from the mergers of stellar-mass black holes, as detected by LIGO-Virgo-Kagra (LVK), especially if they proactively contribute to the dark matter content (Bird et al. 2016; Fakhry et al. 2021, 2022a,b, 2023b; Fakhry & Del Popolo 2023; Fakhry et al. 2023a; Fakhry 2023). However, other studies indicate that the scenario based on the merger of PBHs in the early Universe cannot contribute to the merger events recorded by LVK detectors unless their contribution to dark matter is subpercent (Hall et al. 2020; Hütsi et al. 2021; Chen et al. 2022; Franciolini et al. 2022).

Besides a narrow mass range for PBHs as the single dark matter component, one can consider PBHs with ex-

s.fakhry@sbu.ac.ir

m.farhang@sbu.ac.ir

antonino.delpopolo@unict.it

tended mass distributions and/or scenarios where dark matter consists of various components with distinct masses, interactions and behaviors, such as PBHs and microscopic particles. The former scenario can address challenges such as initial seeds of supermassive black holes (Carr & Silk 2018) and the cored density profiles of dwarf galactic halos (Boldrini et al. 2020). Also, this scenario, with its broad mass range, can potentially provide a more comprehensive explanation for the detection of gravitational wave signals from merging black holes (see, e.g., Sasaki et al. 2018; Martinelli et al. 2022; Bagui & Clesse 2022).

In both scenarios, dark matter is expected to be present during the formation of PBHs where significant primordial density fluctuations play a crucial role. However, it is more common for weaker density fluctuations to occur which do not lead to PBH formation. These fluctuations are large enough to trigger dark matter halo formation before they naturally occur, and therefore these halos have exceptionally dense internal structures. Specifically, the ultradense dark matter halos, or UDMHs, form from the collapse of excessively dense regions in the radiation epoch. It is worth mentioning that dense halos can also form around PBHs, albeit with a different mechanism (Inman & Ali-Haïmoud 2019). The only common aspect between the UDMHs we refer to and PBHs is their shared origin through similar formation processes.

The formation of dark matter halos has been studied through numerical simulations and analytical approaches, specifically targeting those that developed during the matter-dominated era (see, e.g., Gosenca et al. 2017; Delos et al. 2018; White 2022; Del Popolo & Fakhry 2023). On the other hand, halos forming during the radiation-dominated era have the potential to possess significantly higher densities. Several investigations have been carried out to specifically examine the emergence of UDMHs during the radiation-dominated era (see, e.g., Kolb & Tkachev 1994; Dokuchaev & Eroshenko 2002; Berezhinsky et al. 2010, 2013; Nakama et al. 2019).

Motivated by simulations (Blanco et al. 2019), Delos & Silk (2023) introduced an analytical framework to explore the formation and evolution of UDMHs during the radiation-dominated era. This requires definite models for halo mass functions that characterize the distribution of mass among dark matter halos. A large amount of research has been devoted to identifying mass functions that accurately describe the simulations and data of galactic halos (see, e.g., Press & Schechter 1974; Sheth et al. 2001; Sheth & Tormen 2002; Reed et al. 2003, 2005;

Warren et al. 2006; Del Popolo 2006; Tinker et al. 2008; Del Popolo et al. 2017).

In particular, Delos & Silk (2023) used Monte Carlo simulation to get the distribution of first barrier crossings for a Gaussian random walk which led to the Press-Schechter (PS) mass function (Press & Schechter 1974). However, the PS mass function has limitations in accurately describing the mass distribution of dark matter halos, particularly at high redshifts (Del Popolo et al. 2017). The discrepancy can be associated with certain physical effects ignored in the PS formalism which play crucial roles in forecasting halo abundance.

In this study we expand the previous works by taking into account various physical and geometrical modifications to the formation and evolution scenarios of UDMHs. We consider the multicomponent scenario for dark matter, i.e., consisting of particles and possibly PBHs with a broad-mass range. This should be contrasted with the case of dark matter being solely composed of PBHs with masses spanning several orders of magnitude, where the halos, and in particular, UDMHs, would be clusters composed of much smaller PBHs. It is worth noting that the determination of the precise mass spectrum for PBHs can be tricky, which would affect the abundance of UDMHs and PBHs (Chisholm 2011).

The overall structure of this work is outlined as follows. In Section 2 we discuss the formation and evolution of UDMHs during the radiation-dominated era and calculate their abundance with more realistic mass functions and well-motivated primordial power spectra. In Section 3 we present and discuss the results. We conclude in Section 4.

2. ULTRADENSE DARK MATTER HALOS

In this section we investigate the impact of certain physically-motivated modifications to the formation of UDMHs on their mass functions. We also introduce several primordial power spectra for curvature perturbations, either motivated by various scenarios of the early Universe or considered as possible phenomenological extensions to the scale-invariant spectrum. These spectra will later be used as case studies required to calculate the UDMH mass functions.

2.1. Dark matter halo formation

The growth of linear density perturbations of dark matter in the radiation-dominated era, seeded by primordial curvature perturbations ζ , is described by

$$\begin{aligned} \delta(k, a) &= \alpha \zeta(k) \log \left(\beta \frac{a}{a_{\text{H}}} \right) \\ &= \alpha \zeta(k) \log \left(\sqrt{2} \beta \frac{k}{k_{\text{eq}}} \frac{a}{a_{\text{eq}}} \right), \end{aligned} \quad (1)$$

where $a \gg a_H$, with a_H being the scale factor at horizon entry, $k_{\text{eq}} \simeq 0.01 \text{ Mpc}^{-1}$ and $a_{\text{eq}} \simeq 3 \times 10^{-4}$ are respectively the horizon scale and the scale factor at matter-radiation equality. Moreover we have $\alpha = 6.4$, and $\beta = 0.47$ from numerical suggestions (Hu & Sugiyama 1996). Also horizon crossing occurs at

$$\frac{a_H}{a_{\text{eq}}} = \frac{1 + \sqrt{1 + 8(k/k_{\text{eq}})^2}}{4(k/k_{\text{eq}})^2} \simeq \frac{\sqrt{2} k_{\text{eq}}}{2k}, \quad k \gg k_{\text{eq}}. \quad (2)$$

We assume that at horizon crossing non-relativistic dark matter was decoupled from radiation. The trajectories of individual dark matter particles in response to the curvature kick can be modeled by allowing for independent drift along each axis of an ellipsoid. The parameters of eccentricity, e , and prolateness, p , characterize the initial tidal field encountered by a region with a scale k . This would determine the axis ratios governing the ellipsoidal drifting motion. Subsequently, the density evolution within this region would be subject to the contraction or expansion of each axis induced by the particle motion, described by

$$\frac{\rho}{\bar{\rho}_m} = \prod_{i=1}^3 |1 - \lambda_i \delta(k, a)|^{-1}, \quad (3)$$

where $\bar{\rho}_m$ represents the average density of dark matter content. Also, λ_i 's denote the eigenvalues of the deformation tensor in the Zeldovich approximation, which can be obtained as

$$\lambda_1 = \frac{1 + 3e + p}{3}, \quad \lambda_2 = \frac{1 - 2p}{3}, \quad \lambda_3 = \frac{1 - 3e + p}{3}. \quad (4)$$

Along any given axis i , collapse occurs when the linear density perturbation $\delta(k, a)$ grows to exceed λ_i^{-1} . The axis with the smallest eigenvalue will be the last to collapse. Labeling this smallest eigenvalue by λ_3 , the entire ellipsoidal region will collapse once $\lambda_3 \delta(k, a_c) = 1$, where a_c refers to the collapse scale factor. Under these conditions, the critical density contrast can be determined as

$$\delta_c = \frac{3}{1 - 3e + p}. \quad (5)$$

In Sheth et al. (2001) it is demonstrated that in a Gaussian random field with a density contrast δ and a linear root-mean-square σ , the most probable values for eccentricity and prolateness would be $e_{\text{mp}} = \sigma/(\sqrt{5}\delta)$ and $p_{\text{mp}} = 0$, respectively. These most probable values give the collapse threshold $\delta_c = 3(1 + \sigma/\sqrt{5})$, which in the excursion set formalism translates into the moving barrier $B(S) = 3(1 + \sqrt{S/5})$ with $S \equiv \sigma^2$ (Bond et al. 1991). Therefore, if the density is high enough, the collapse will occur during the radiation-dominated era.

Within the above collapse scenario one can demonstrate with a quantitative example how UDMHs would abundantly outnumber PBHs if formed from similar-scale density perturbations. Considering a typical 3σ density peak with $e \simeq 0.15$, its collapse threshold is $\delta_c \simeq 5$. Collapse by $a = 10 a_H$ requires an extreme curvature perturbation $\zeta \geq 0.5$, while collapse by $a = 300 a_H$ needs only a milder $\zeta \geq 0.15$. On the other hand, PBH formation requires the utmost density spikes with $\zeta \sim 1$ (Green et al. 2004). Therefore, common mild perturbations can form abundant UDMHs, while only the rarest spikes are qualified to form PBHs.

One should note that halos are not guaranteed to form from collapsed structures in the radiation-dominated epoch. It has been shown by numerical simulations that a peak's collapse leads to the formation of a virialized halo only when the collapsed area becomes locally matter-dominated (Blanco et al. 2019). On the other hand, the collapsed regions are found to be orders of magnitude denser than the dark matter background, with their densities scaling as $\sim e^{-2} \bar{\rho}_m$ (Delos & Silk 2023). Given the standard ellipticity $e \sim 0.15$ of the tidal field at a 3σ peak, local matter dominance occurs at $a/a_{\text{eq}} \sim e^2 \simeq \mathcal{O}(10^{-2})$. This results in the formation of a halo well before the onset of matter domination. The density within these halos would be exceptionally high as they scale with the mean cosmic density at their formation time.

2.2. Dark matter halo mass functions

The excursion set theory provides the unconditional mass function of halos, which describes the average comoving number density of halos within a logarithmic mass interval (Bond et al. 1991),

$$\frac{dn}{d \log M} = \frac{\bar{\rho}_{m,0}}{M} \left| \frac{d \log \nu}{d \log M} \right| \nu f(\nu). \quad (6)$$

Here, $\bar{\rho}_{m,0} \simeq 33 \text{ M}_\odot/\text{kpc}^3$ denotes the comoving average density of dark matter content, and $\nu \equiv \delta_c/\sigma$ is a dimensionless parameter known as peak height. Also, the function $f(\nu)$, known as the ‘‘multiplicity function’’, represents the distribution of first crossings. As previously stated, $\sigma(M, a)$ represents the root-mean-square of linear density fluctuations smoothed on the mass scale M , i.e.,

$$\sigma^2(M, a) = \frac{1}{2\pi^2} \int_0^\infty P(k, a) W^2(k, M) k^2 dk, \quad (7)$$

where $P(k, a)$ refers to the power spectrum of linear matter fluctuations and $W(k, M)$ is the smoothing window

function, assumed to be a sharp- k filter¹ (Bond et al. 1991),

$$W(k, M) = \begin{cases} 1 & \text{if } 0 < k \leq k_M \\ 0 & \text{otherwise} \end{cases} \quad (8)$$

with $k_M = (6\pi^2 \bar{\rho}_{m,0}/M)^{1/3}$ (Lacey & Cole 1994). Under such conditions we have

$$\frac{d \log \nu}{d \log M} = \frac{k_M^3 P(k_M, a)}{12\pi^2 \sigma^2(M, a)}. \quad (9)$$

From Eq. (1) one gets

$$P(k, a) = \frac{2\pi^2 \alpha^2}{k^3} \left[\log \left(\sqrt{2}\beta \frac{k}{k_{\text{eq}}} \frac{a}{a_{\text{eq}}} \right) \right]^2 P_\zeta(k), \quad (10)$$

where $P_\zeta(k)$ is the dimensionless power spectrum of primordial curvature perturbations. The exact form of $P_\zeta(k)$ depends on the assumed inflationary scenario that seeds the perturbations. We will provide some suggestions in Section 2.3.

Our main goal in this work is to explore the role of certain physical factors in the halo mass function in the ultradense regime within the excursion set theory, through their impact on the dynamical barrier. In scenarios with different types of barriers, the distribution of first crossings can be determined by simulating a significant number of random walks (Sheth 1998; Sheth & Tormen 2002). In Sheth & Tormen (2002) it is shown that, for a wide range of dynamical barriers, the initial crossing distribution can be approximated by

$$f(S) = |T(S)| \exp\left(-\frac{B(S)^2}{2S}\right) \frac{1}{S\sqrt{2\pi S}}, \quad (11)$$

where $T(S)$ can be obtained by employing a Taylor expansion of $B(S)$

$$T(S) = \sum_{n=0}^5 \frac{(-S)^n}{n!} \frac{\partial^n B}{\partial S^n}. \quad (12)$$

Delos & Silk (2023) derive an approximation for the distribution of first barrier crossings within a Gaussian random walk framework, validated by Monte Carlo simulation,

$$f(S) \approx \frac{3 + 0.556\sqrt{S}}{\sqrt{2\pi S^3}} \exp\left(-\frac{B^2}{2S}\right) \left(1 + \frac{S}{400}\right)^{-0.15}, \quad (13)$$

¹ For the small-scale power spectrum we are interested in, employing a real-space top-hat window function with a truncated power spectrum may result in specific issues, such as increased variance even for masses below the cutoff scale. This can be addressed by utilizing the sharp- k window function (Tokeshi et al. 2020; Sabti et al. 2022; Alkhanishvili et al. 2023).

which corresponds to the PS multiplicity function²,

$$[\nu f(\nu)]_{\text{PS}} = \sqrt{\frac{2}{\pi}} \frac{(\nu + 0.556) \exp[-0.5(1 + \nu^{1.34})^2]}{(1 + 0.0225\nu^{-2})^{0.15}}. \quad (14)$$

There are, however, discrepancies between the predictions of the PS mass function and dark matter halo distributions, especially at high redshifts (Del Popolo et al. 2017). The disagreements, as already stated, might be attributed to various physical factors ignored in the PS formalism and may have a non-negligible impact on the abundance of UDMHs. The first factor considered here is geometrical in nature and generalizes the spherical-collapse model in the essence of PS formalism to ellipsoidal-collapse halo models. The modified mass function is known as Sheth-Tormen (ST), described by (Sheth et al. 2001)

$$[\nu f(\nu)]_{\text{ST}} = A_1 \sqrt{\frac{2\nu'}{\pi}} \left(1 + \frac{1}{\nu'^q}\right) \exp\left(-\frac{\nu'}{2}\right), \quad (15)$$

where $q = 0.3$, $\nu' \equiv 0.707\nu^2$, and $A_1 = 0.322$ is determined by demanding that the integral of $f(\nu)$ across all possible values of ν equals unity.

Besides the geometric conditions during the virialization process of dark matter halos, other physical factors can also impact the collapse of overdense regions and, consequently, the halo mass function. Incorporating these essential physical factors into the analysis is crucial as they capture the genuine physics governing halo collapse and growth and the processes underlying structure formation and evolution throughout cosmic history. Additionally, this approach allows the collapse threshold to depend on effective physical factors. As a result, the barrier adjusts accordingly with these variables, resulting in a more realistic model for halo collapse. Among these corrections, we consider the impact of angular momentum, dynamical friction, and cosmological constant on the halo mass function. These corrections are shown to play a role in reducing the discrepancies, particularly in controversial mass ranges. Including the effect of angular momentum and cosmological constant, the mass function (Del Popolo 2006), referred to as DP1 in this work, is found to be

$$[\nu f(\nu)]_{\text{DP1}} \approx A_2 \sqrt{\frac{\nu'}{2\pi}} k(\nu') \exp\{-0.4019\nu' l(\nu')\}, \quad (16)$$

² The statement explains how the multiplicity function $f(\nu)$ is connected to the first crossing distribution $f(S, t)$. The latter represents the probability distribution for the first time a random walk crosses a specific barrier $B(S)$. The equation $\nu f(\nu) = S f(S, t)$ demonstrates that $f(\nu)$ can be derived from $f(S, t)$, illustrating a fundamental relation within the excursion set theory (Zentner 2007).

with $A_2 = 0.974$ set by normalization, and

$$k(\nu') = \left(1 + \frac{0.1218}{(\nu')^{0.585}} + \frac{0.0079}{(\nu')^{0.4}} \right), \quad (17)$$

and

$$l(\nu') = \left(1 + \frac{0.5526}{(\nu')^{0.585}} + \frac{0.02}{(\nu')^{0.4}} \right)^2. \quad (18)$$

The influence of dynamical friction on the barrier was also investigated in [Del Popolo et al. \(2017\)](#), leading to the (hereafter DP2) mass function,

$$[\nu f(\nu)]_{\text{DP2}} \approx A_3 \sqrt{\frac{\nu'}{2\pi}} m(\nu') \exp\{-0.305\nu'^{2.12}n(\nu')\}, \quad (19)$$

where $A_3 = 0.937$ is set by normalization, and we have

$$m(\nu') = \left(1 + \frac{0.1218}{(\nu')^{0.585}} + \frac{0.0079}{(\nu')^{0.4}} + \frac{0.1}{(\nu')^{0.45}} \right), \quad (20)$$

and

$$n(\nu') = \left(1 + \frac{0.5526}{(\nu')^{0.585}} + \frac{0.02}{(\nu')^{0.4}} + \frac{0.07}{(\nu')^{0.45}} \right)^2. \quad (21)$$

We will use these mass functions in Section 3 to calculate the abundance of UDMHs for various primordial power spectra introduced in the next section.

2.3. Primordial power spectra

Formation of PBHs and UDMHs in the radiation-dominated era requires substantial amplification (of the order of $\mathcal{O}(10^7)$) of the primordial power spectrum on small scales compared to the observationally-supported almost scale-invariant spectrum on large scales. We therefore consider modifications to this scale-invariant spectrum, $P_{\zeta_0}(k)$, by some large-amplitude fluctuations on small scales, P_{ζ_1} , i.e.,

$$P_{\zeta}^x(k) = P_{\zeta_0}(k) + P_{\zeta_1}^x(k), \quad (22)$$

where $P_{\zeta}^x(k)$ is the total spectrum, “x” stands for the different models used, and

$$P_{\zeta_0} = A_0 \left(\frac{k}{k_{p_0}} \right)^{n_s-1}. \quad (23)$$

Here $k_{p_0} = 5 \times 10^{-2} \text{ Mpc}^{-1}$ is the scalar pivot scale and $A_0 = 2.1 \times 10^{-9}$ and $n_s = 0.96$ are set from cosmic microwave background observations ([Planck Collaboration et al. 2020](#)).

In this work, we explore four models for $P_{\zeta_1}^x(k)$ with different features to allow for PBH and UDMH formation on various mass scales.

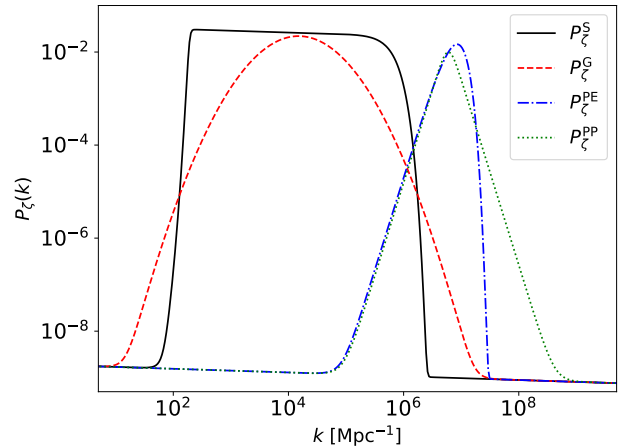


Figure 1. Primordial power spectra as a function of k for the four models introduced in Section 2.3. The (black) solid, (red) dashed, (blue) dot-dashed, and (green) dotted lines correspond to the spectrum described by Eq. 22, with the amplifications given by Eqs. (24), (26), (27), and (28), respectively. The characteristic scales are chosen to be $k_1 = 190 \text{ Mpc}^{-1}$ for P_{ζ}^S , $1.5 \times 10^4 \text{ Mpc}^{-1}$ for P_{ζ}^G , and $6 \times 10^6 \text{ Mpc}^{-1}$ for P_{ζ}^{PE} and P_{ζ}^{PP} . The small-scale amplitude of all power spectra is set to be $A_1 = 10^{-2}$.

As the first extension, we consider a smooth transition from large- to small-scale spectrum, also assumed to be nearly scale-invariant on these scales,

$$P_{\zeta_1}^S = A_1 \left(\frac{k}{k_{p_1}} \right)^{n_s-1} D(k, k_1, w) \exp \left[\frac{-(k - k_2)^2}{2\sigma^2} \right], \quad (24)$$

where $k_{p_1} = 10^6 \text{ Mpc}^{-1}$ and $A_1 \approx 2.2 \times 10^{-2}$ are chosen as the pivot scale and amplitude for the small-scale power spectrum, and we have defined

$$D(k, k_1, w) = \frac{1}{2} \left[1 + \tanh \left(\frac{k - k_1}{w} \right) \right], \quad (25)$$

as the smoothing function with the transition scale $k_1 \simeq 190 \text{ Mpc}^{-1}$ and width $w = 15 \text{ Mpc}^{-1}$. The Gaussian function is used to smoothly kill the amplified fluctuations on very small scales beyond the cut-off wavenumber $k_2 \simeq 6 \times 10^4 \text{ Mpc}^{-1}$ with a width $\sigma = 2 \times 10^5 \text{ Mpc}^{-1}$. The maximum mass of UDMHs seeded by this power spectrum would then be automatically set to $\sim 10^5 M_{\odot}$.

As the second extension, we model a localized amplification of the power spectrum in the k -space with a Gaussian bump,

$$P_{\zeta_1}^G = A_1 \exp \left(\frac{-\log(k/k_1)^2}{2\sigma^2} \right), \quad (26)$$

where the bump is centred at $k_1 = 1.5 \times 10^4 \text{ Mpc}^{-1}$ with width $\sigma = 1.2$ and amplitude $A_1 = 10^{-2}$.

As the third model we consider a certain combination of power-law and exponential function as (Delos & Franciolini 2023)

$$P_{\zeta_1}^{\text{PE}}(k) = A_1 \left(\frac{k}{k_1}\right)^4 \exp\left[1 - \left(\frac{k}{k_1}\right)^2\right], \quad (27)$$

where $A_1 = P_{\zeta_1}^{\text{PE}}(k_1)$ is the amplitude of the spectrum at the characteristic scale k_1 . The spectrum experiences an expansion proportional to k^4 for $k < k_1$, representing the distinctive steep growth observed in conventional ultraslow-roll inflation scenarios (Byrnes et al. 2019; Franciolini & Urbano 2022; Karam et al. 2023). For $k > k_1$ the spectrum undergoes damping.

The last case we consider is constructed from combination of two power-laws as

$$P_{\zeta_1}^{\text{PP}}(k) = 2A_1 \left[\left(\frac{k}{k_1}\right)^{-4} + \left(\frac{k}{k_1}\right)^4 \right]^{-1}, \quad (28)$$

with a damping tail different from P_{ζ}^{PE} . Figure 1 illustrates the four power spectra introduced in this section. As can be seen, the amplitudes are chosen so that the spectra are amplified to $\sim 10^{-2}$ at the characteristic scale k_1 of each model.

3. RESULTS AND DISCUSSIONS

In this section we present and compare the estimated abundance of UDMHs based on the modifications to halo formation processes discussed in Section 2.2. Figures 2–5 illustrate the differential mass fraction $df/d\log M = (M/\bar{\rho}_{m,0})(dn/d\log M)$ of UDMHs as a function of mass M in the radiation-dominated epoch, i.e., $a \leq a_{\text{eq}}$, with the various models of primordial power spectra of Section 2.3. We have considered three distinct halo mass functions: the ST approximation, and DP1 and DP2 formulations, which are compared to the results from the PS formalism.

Figure 2 corresponds to the power spectrum with the smooth transition described by Eq. (22). It should be noted that the mass function of collapsed regions at early epochs of $a = 10^{-7}$ and 10^{-6} are plotted only for the sake of comparison, as local matter dominance, required for halos to form in a radiation-dominated Universe, is not expected to occur before $a/a_{\text{eq}} \simeq \mathcal{O}(10^{-2})$. As can be seen, the DP1, ST and DP2 mass functions yield a higher abundance of large-mass UDMHs ($M \geq 10^4 M_{\odot}$) when compared to the PS mass function, with DP1 predicting the highest abundance for these halos. This illustrates the impact of corrections due to angular momentum as the main physical factor considered in the DP1 scenario, since the cosmological constant is not expected

to play a significant role in the early Universe. Including dynamical friction, on the other hand, reduces the formation of these dense halos, as is visible from the DP2 curve. The ST mass function, with its incorporation of triaxial collapse in the halo formation scenario, seems to maintain a rigorous standard and falls in between the previous two.

For comparison, we have plotted observational constraints on the PBH abundance in the mass range of interest against the predicted UDMH mass functions, including microlensing constraints from EROS and OGLE (Tisserand et al. 2007; Niikura et al. 2019), scalar-induced GWs with NANOGrav (Chen et al. 2020), direct constraints on PBH mergers with LIGO detector (Abbott et al. 2019, 2022), the stochastic background of PBH mergers with LIGO detector (Chen & Huang 2020), microlensing of GWs by PBHs (Jung & Shin 2019), and constraints from the disruption of ultra-faint dwarfs (UFD) (Brandt 2016). We see that the UDMHs in this scenario are expected to have significant abundance particularly in the large-mass tail of the mass spectrum, even in the regions already observationally excluded for PBHs by data. It should be highlighted that the higher number of UDMHs formed during the radiation-dominated era, in comparison to PBHs, is also mentioned in Ricotti & Gould (2009); Kohri et al. (2014). In addition, the mass functions in all of the halo formation models turn out to have their peaks at around the same mass ($M \simeq 10^5 M_{\odot}$, imposed by the transition scales $k = 190 \text{ Mpc}^{-1}$). The DP1 mass function is predicted to have the highest peak, several times larger than the PS prediction. The sudden decrease in the low-mass tail of the mass functions is due to the large- k cutoff in the power spectrum.

Figure 3 illustrates the predicted mass function for the UDMHs in a Universe with the Gaussian modification of Eq. (26) in its primordial scalar power spectrum. The Gaussian bump enables the exploration of UDMH formation across different mass scales, based on the location of the peak in the power spectrum. As the scale factor increases to $a = a_{\text{eq}}$, the differential mass fraction shifts towards higher masses for all mass functions. For the case considered in this work, i.e., with the bump centred at $k_1 = 1.5 \times 10^4 \text{ Mpc}^{-1}$, the peaks of the UDMH mass functions at $a = a_{\text{eq}}$ happen at $M \simeq 10^3 M_{\odot}, 5 \times 10^2 M_{\odot}, 2 \times 10^2 M_{\odot}$, and $10^2 M_{\odot}$ for the DP1, ST, DP2 and PS models, respectively. The results also show significant contributions for the UDMHs in the large M -tail, with the DP1 having the highest contribution, again mainly in the regions excluded for PBHs.

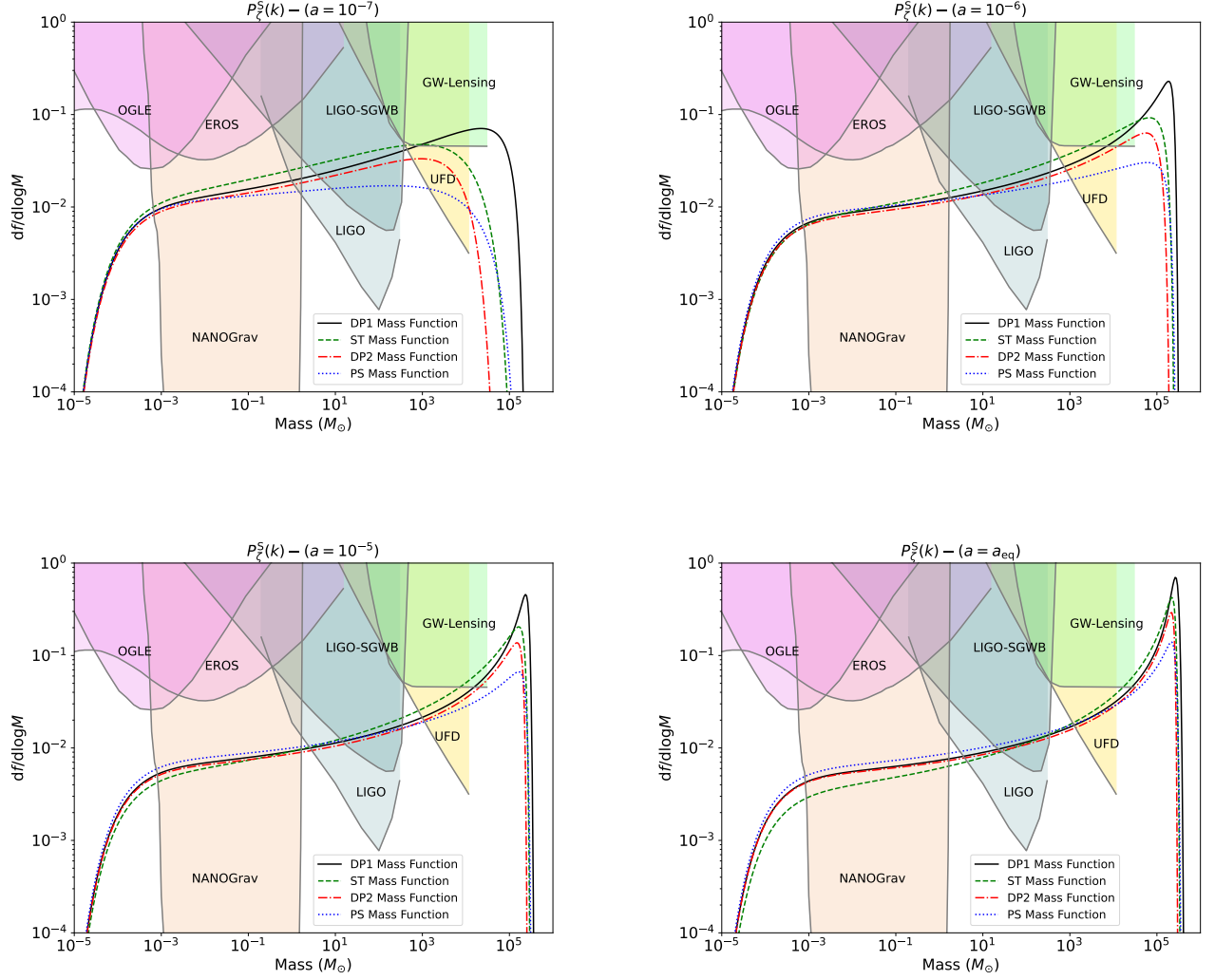


Figure 2. Differential dark matter mass fraction in UDMHs for different scale factors ($a \leq a_{\text{eq}}$), seeded by primordial perturbations described by the power spectrum $P_{\zeta}^S(k)$. The (black) solid, (green) dashed, (red) dot-dashed, and (blue) dotted lines represent the results for DP1, ST, DP2, and PS mass functions. Observational constraints on PBHs are plotted to compare the predicted abundance of UDMHs and the upper limits on PBHs with similar mass scales. The constraints are based on the results from microlensing data by EROS (Tisserand et al. 2007), the disruption of ultra-faint dwarfs (UFD) (Brandt 2016), microlensing of GWs by PBHs (GW-Lensing) (Jung & Shin 2019), microlensing data by OGLE (Niikura et al. 2019), stochastic background of PBH mergers with LIGO (LIGO-SGWB) (Chen & Huang 2020), scalar-induced GWs with NANOGrav (Chen et al. 2020), and direct constraints on PBH-PBH mergers with LIGO (Abbott et al. 2019, 2022).

Figures 4 and 5 illustrate the mass function of smaller-mass UDMHs, seeded by fluctuations described by the power spectra of Eqs. (27) and (28) respectively. Given the remarkably high internal density of UDMHs formed on smaller scales, their evolution is expected to be minimally affected by the scale factor. Therefore, for these two cases, we set $a = a_{\text{eq}}$ in the calculations for convenience.

Figure 4 illustrates the differential dark matter mass fraction in UDMHs, calculated for the $P_{\zeta}^{\text{PE}}(k)$ as the

primordial power spectrum with various amplitudes A_1 , corresponding to $P_{\zeta}^{\text{PE}}(k_1) = 10^{-1}, 10^{-2}$ and 10^{-3} at the characteristic scale $k_1 = 6 \times 10^6 \text{ Mpc}^{-1}$. The results are shown for the predictions of the three different halo formation scenarios ST, DP1, and DP2, compared against the PS mass function.

The plots show that the DP1 scenario has the largest overall contribution to dark matter compared to ST, DP2 and PS. Also, the predicted mass for the largest halos to form in DP1 is significantly (\sim an order of mag-

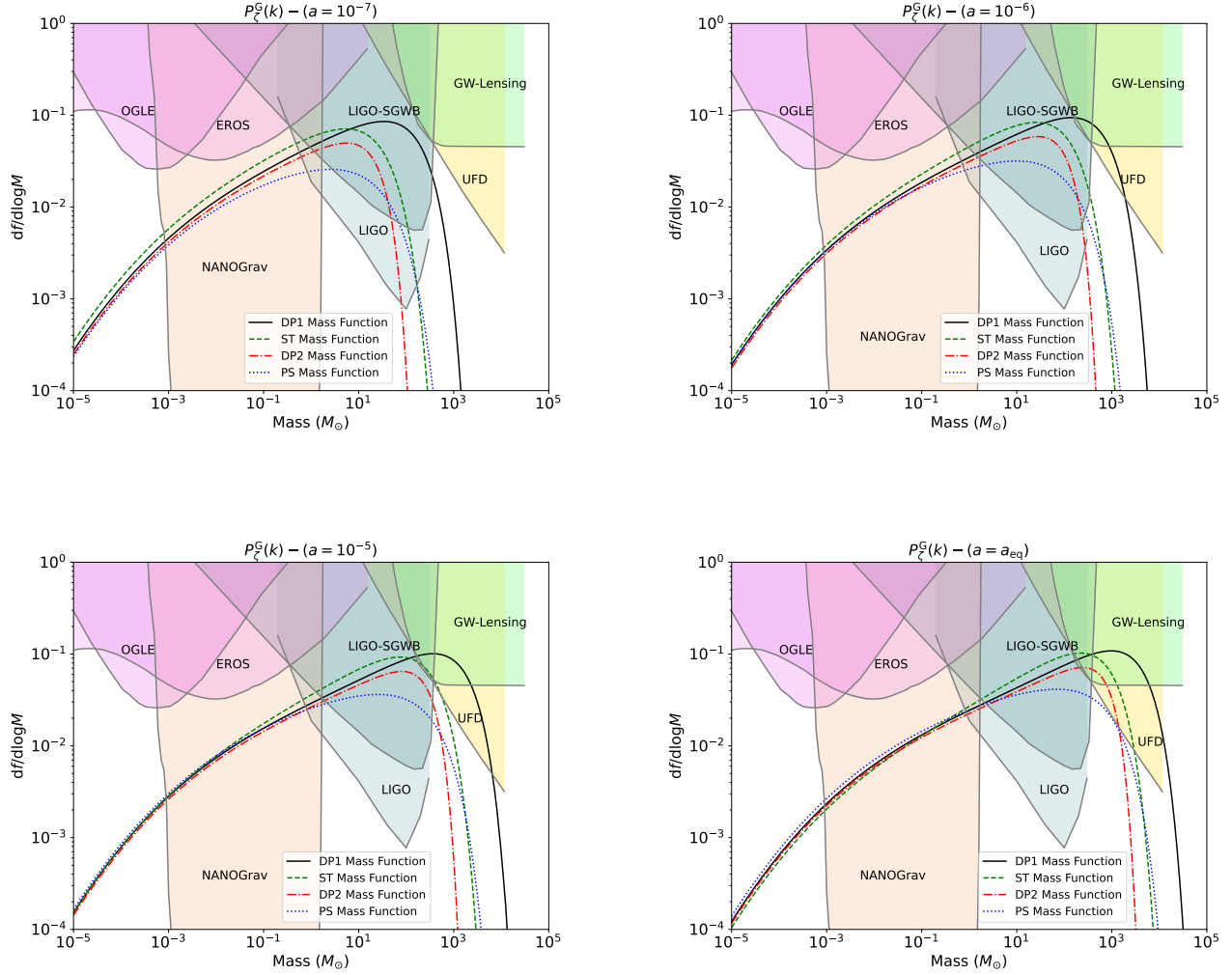


Figure 3. Similar to Figure 2 but with $P_\zeta^G(k)$ as the primordial power spectrum.

nitude) higher than the expected maximum mass in the other three formalisms. We also find that this maximum mass in each model decreases as the amplitude $P_\zeta^{\text{PE}}(k_1)$ drops from 10^{-1} to 10^{-3} . This is expected as with lower amplitudes for the perturbations that would seed dense halos, the chances of their formation would decrease.

For the sake of comparison, the observational bounds on the PBH abundance are also plotted in this mass range, including the microlensing constraints from the Hyper-Supreme Cam (HSC) (Croon et al. 2020), PBH-induced motions in pulsar timing arrays (Dror et al. 2019), microlensing constraints from Kepler (Griest et al. 2014), microlensing constraints from EROS (Tisserand et al. 2007), and neutron star capture and destruction (Capela et al. 2013). These UDMHs are expected to form with abundances which are ruled out by data for PBHs with the same masses.

Similar calculations have been performed for the $P_\zeta^{\text{PP}}(k)$ for the primordial power spectrum and the results are presented in Figure 5. The mass functions show deviations in the low-mass tail from the predictions for the $P_\zeta^{\text{PE}}(k)$ spectrum, and are damped with relatively shallower slopes. Apart from this, the overall behaviour of the mass functions are similar to the results of Figure 4.

In this work we have focused on adiabatic curvature perturbations. However, it is worth noting that isocurvature perturbations in radiation-dominated era can lead to the formation of UDMHs, in an even more favorable way (Kolb & Tkachev 1994). That is because with adiabatic curvature perturbations, local matter domination is required for UDMHs to form, while PBHs can emerge from radiation fluctuations alone. With isocur-

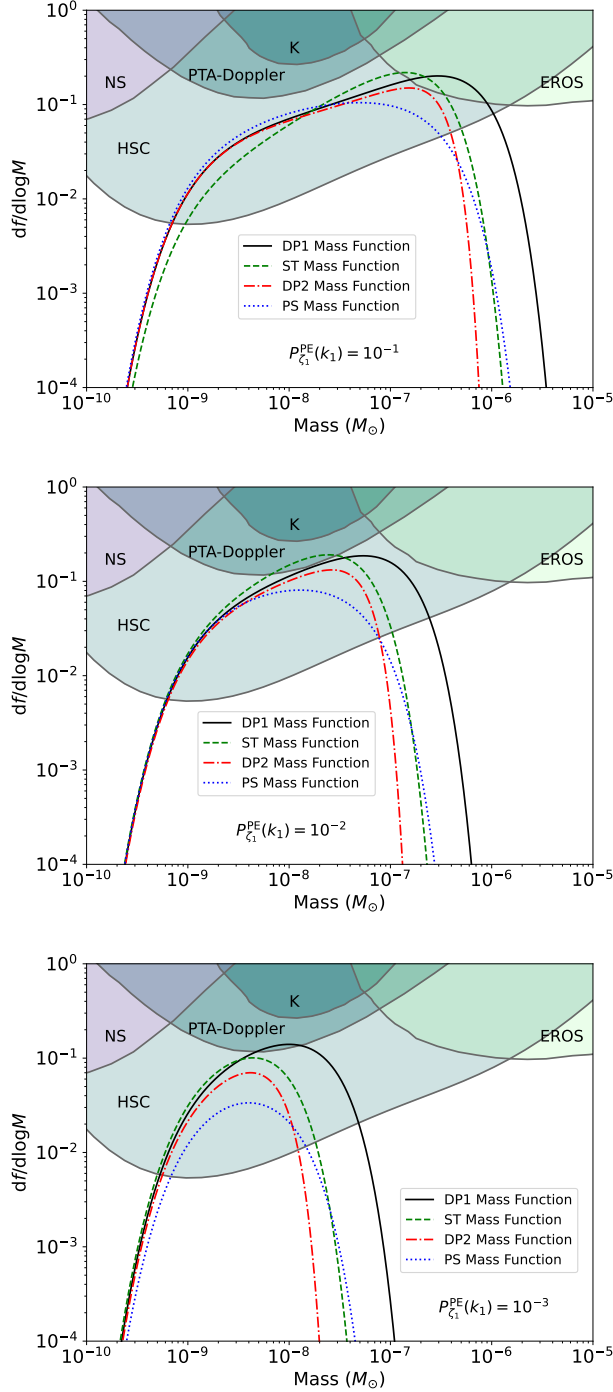


Figure 4. Differential mass fraction in UDMHs as a function of mass M , with $P_{\zeta}^{\text{PE}}(k)$ as the primordial power spectrum, and for different primordial amplitudes (from top to bottom: $P_{\zeta_1}^{\text{PE}}(k_1) = 10^{-1}, 10^{-2}$ and 10^{-3} , respectively). The (black) solid, (green) dashed, (red) dot-dashed, and (blue) dotted lines correspond to the results for DP1, ST, DP2, and PS mass functions. The characteristic scale k_1 is set to $6 \times 10^6 \text{ Mpc}^{-1}$. For comparison with the bounds on the PBH abundance, observational constraints are also plotted, including microlensing constraints from EROS (Tisserand et al. 2007), neutron star capture and destruction (NS) (Capela et al. 2013), microlensing constraints from Kepler (K) (Griest et al. 2014), PBH-induced motions in pulsar timing arrays (PTA-Doppler) (Dror et al. 2019), and microlensing constraints from HSC (Croon et al. 2020).

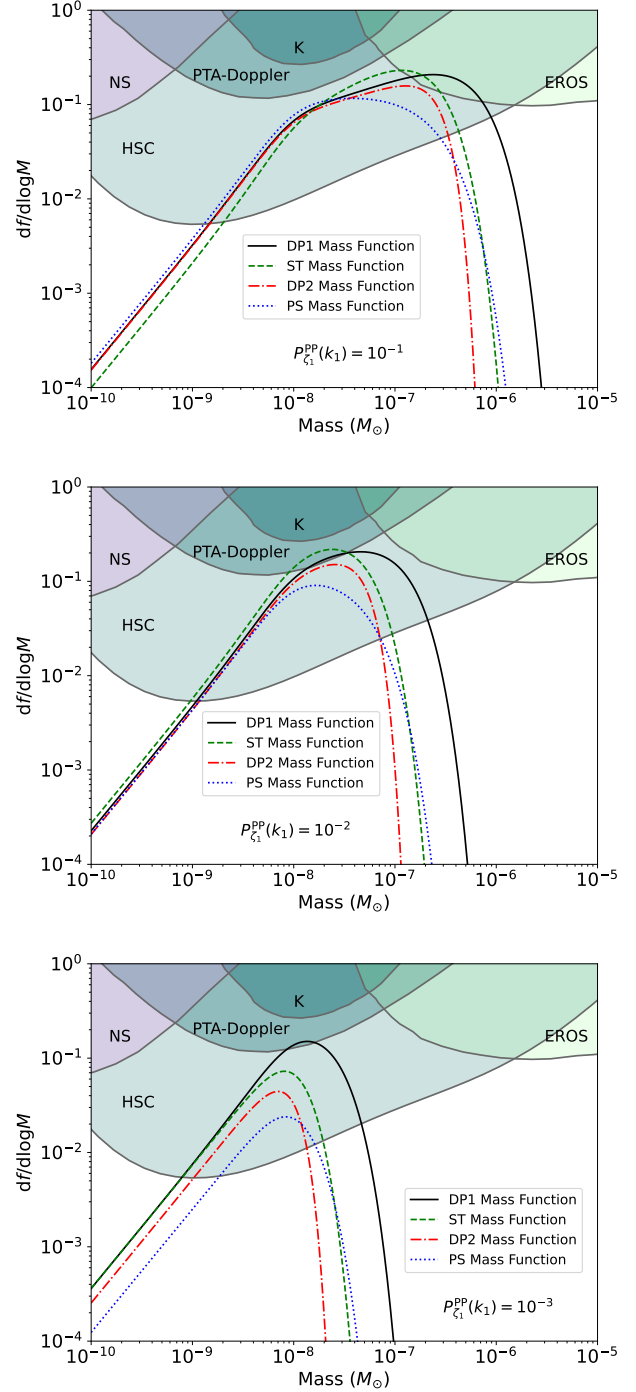


Figure 5. Similar to Figure 4 but with $P_{\zeta}^{\text{PP}}(k)$ as the primordial power spectrum.

vature perturbations, on the other hand, both PBHs and halos essentially originate from matter perturbations.

Ultimately, one can expect UDMHs to persist throughout the evolution of the Universe. This stems from the fact that their internal structure is unlikely to be significantly altered by subsequent accretion of mat-

ter (Delos & White 2023). Furthermore, their exceptionally high density, i.e., $\rho \sim 10^{12} M_{\odot}/\text{pc}^3$, grants them substantial resistance to phenomena such as tidal stripping within larger structures like galactic halos (Stücker et al. 2023). It has also been argued that the infrequent UDMH mergers are unlikely to impact the halos' mass fraction and their characteristic internal density values (Drakos et al. 2019; Delos et al. 2019).

4. CONCLUSIONS

Primordial black holes, originating from substantial density fluctuations, could have a mass distribution spanning several orders of magnitude. In such scenarios, analogous yet less intense, primordial density fluctuations might give rise to an abundance of UDMHs that form alongside PBHs. Having formed early in the radiation-dominated era, these halos are predicted to be highly dense, i.e., about 10^{12} times denser than regular cold dark matter halos. Their high density makes them resistant to tidal disruption.

In this work we investigated the formation and evolution of UDMHs in the radiation-dominated epoch. We employed analytical modelling based on the excursion set theory to calculate their abundance. Specifically, we derived the halo mass functions using DP1, DP2 and ST formulations, considering physical factors such as angular momentum, dynamical friction, cosmological constant and triaxial collapse geometry and compared the results with the PS forecasts. The calculations were carried out for four primordial power spectra, with different amplification patterns at specific scales. The power spectra have been chosen to cover subsolar, stellar, and intermediate-mass ranges for UDMHs.

The results demonstrate higher abundance of UDMHs predicted by the more realistic mass functions considered in this work compared to the PS formalism which

highlights the importance of these physical and geometrical factors. In particular the DP1 formulation leads to the highest abundance of UDMHs, as well as predicting the highest maximum mass, for a given primordial power spectrum, compared to the other three formalisms. This implies that angular momentum has a significant impact on halo formation. On the other hand, the decrease in the halo abundance for the DP2 mass function suggests the suppression of halo formation due to dynamical friction, although it is still higher than the predictions by the over-simplified PS mass function. The ST mass function, which accounts for triaxial collapse geometry, yield an intermediate abundance between DP1 and DP2 formulations.

Comparison with the current bounds on PBH abundance from different observations suggests that UDMHs are expected to outnumber PBHs at similar mass scales. This result is expected to hold, irrespective of the primordial power spectrum, as the power spectra considered in this work cover different scales and have different characteristics. Our results highlight the importance of accurate analytical approaches for better understanding of UDMH formation. This is particularly important as these halos are expected to survive throughout cosmic time, potentially existing as components of present-day dark matter structures since the early Universe. The forecasted increase in their abundance can significantly alter PBH scenario predictions. Future observations have the potential to detect these halos and thereby provide a means to test hypotheses regarding PBH production in the early Universe. Therefore, the prevalence of UDMHs necessitates a re-examination of PBH constraints and predictions across various mass ranges.

ACKNOWLEDGEMENTS

S.F. would like to acknowledge the Research Council of Shahid Beheshti University.

REFERENCES

- Abbott, B. P., Abbott, R., Abbott, T. D., et al. 2019, Phys. Rev. D, 100, 024017, doi: [10.1103/PhysRevD.100.024017](https://doi.org/10.1103/PhysRevD.100.024017)
- Abbott, R., Abbott, T. D., Acernese, F., et al. 2022, Phys. Rev. Lett., 129, 061104, doi: [10.1103/PhysRevLett.129.061104](https://doi.org/10.1103/PhysRevLett.129.061104)
- Alkhanishvili, D., Porciani, C., & Sefusatti, E. 2023, A&A, 669, L2, doi: [10.1051/0004-6361/202245156](https://doi.org/10.1051/0004-6361/202245156)
- Bagui, E., & Clesse, S. 2022, Phys. Dark Universe, 38, 101115, doi: [10.1016/j.dark.2022.101115](https://doi.org/10.1016/j.dark.2022.101115)
- Belotsky, K. M., Dokuchaev, V. I., Eroshenko, Y. N., et al. 2019, Eur. Phys. J. C, 79, 246, doi: [10.1140/epjc/s10052-019-6741-4](https://doi.org/10.1140/epjc/s10052-019-6741-4)
- Berezinsky, V., Dokuchaev, V., Eroshenko, Y., Kachelrieß, M., & Solberg, M. A. 2010, Phys. Rev. D, 81, 103529, doi: [10.1103/PhysRevD.81.103529](https://doi.org/10.1103/PhysRevD.81.103529)
- Berezinsky, V. S., Dokuchaev, V. I., & Eroshenko, Y. N. 2013, J. Cosmol. Astropart. Phys, 2013, 059, doi: [10.1088/1475-7516/2013/11/059](https://doi.org/10.1088/1475-7516/2013/11/059)
- Bird, S., Cholis, I., Muñoz, J. B., et al. 2016, Phys. Rev. Lett., 116, 201301, doi: [10.1103/PhysRevLett.116.201301](https://doi.org/10.1103/PhysRevLett.116.201301)
- Blanco, C., Delos, M. S., Erickcek, A. L., & Hooper, D. 2019, Phys. Rev. D, 100, 103010, doi: [10.1103/PhysRevD.100.103010](https://doi.org/10.1103/PhysRevD.100.103010)

- Boldrini, P., Miki, Y., Wagner, A. Y., et al. 2020, MNRAS, 492, 5218, doi: [10.1093/mnras/staa150](https://doi.org/10.1093/mnras/staa150)
- Bond, J. R., Cole, S., Efstathiou, G., & Kaiser, N. 1991, APJ, 379, 440, doi: [10.1086/170520](https://doi.org/10.1086/170520)
- Brandt, T. D. 2016, APJL, 824, L31, doi: [10.3847/2041-8205/824/2/L31](https://doi.org/10.3847/2041-8205/824/2/L31)
- Byrnes, C. T., Cole, P. S., & Patil, S. P. 2019, J. Cosmol. Astropart. Phys., 2019, 028, doi: [10.1088/1475-7516/2019/06/028](https://doi.org/10.1088/1475-7516/2019/06/028)
- Cai, R.-G., Chen, T., Wang, S.-J., & Yang, X.-Y. 2023, J. Cosmol. Astropart. Phys., 2023, 043, doi: [10.1088/1475-7516/2023/03/043](https://doi.org/10.1088/1475-7516/2023/03/043)
- Capela, F., Pshirkov, M., & Tinyakov, P. 2013, Phys. Rev. D, 87, 123524, doi: [10.1103/PhysRevD.87.123524](https://doi.org/10.1103/PhysRevD.87.123524)
- Carr, B., Clesse, S., Garcia-Bellido, J., & Kuhnel, F. 2019, arXiv e-prints, arXiv:1906.08217, doi: [10.48550/arXiv.1906.08217](https://doi.org/10.48550/arXiv.1906.08217)
- Carr, B., Kohri, K., Sendouda, Y., & Yokoyama, J. 2021, Rep. Prog. Phys., 84, 116902, doi: [10.1088/1361-6633/ac1e31](https://doi.org/10.1088/1361-6633/ac1e31)
- Carr, B., & Kuhnel, F. 2021, arXiv e-prints, arXiv:2110.02821, doi: [10.48550/arXiv.2110.02821](https://doi.org/10.48550/arXiv.2110.02821)
- Carr, B., & Silk, J. 2018, MNRAS, 478, 3756, doi: [10.1093/mnras/sty1204](https://doi.org/10.1093/mnras/sty1204)
- Chen, Z.-C., & Huang, Q.-G. 2020, J. Cosmol. Astropart. Phys., 2020, 039, doi: [10.1088/1475-7516/2020/08/039](https://doi.org/10.1088/1475-7516/2020/08/039)
- Chen, Z.-C., Yuan, C., & Huang, Q.-G. 2020, Phys. Rev. Lett., 124, 251101, doi: [10.1103/PhysRevLett.124.251101](https://doi.org/10.1103/PhysRevLett.124.251101)
- . 2022, Phys. Lett. B, 829, 137040, doi: [10.1016/j.physletb.2022.137040](https://doi.org/10.1016/j.physletb.2022.137040)
- Chisholm, J. R. 2011, Phys. Rev. D, 84, 124031, doi: [10.1103/PhysRevD.84.124031](https://doi.org/10.1103/PhysRevD.84.124031)
- Croon, D., McKeen, D., Raj, N., & Wang, Z. 2020, Phys. Rev. D, 102, 083021, doi: [10.1103/PhysRevD.102.083021](https://doi.org/10.1103/PhysRevD.102.083021)
- Del Popolo, A. 2006, APJ, 637, 12, doi: [10.1086/498295](https://doi.org/10.1086/498295)
- Del Popolo, A., & Fakhry, S. 2023, Phys. Dark Universe, 41, 101259, doi: [10.1016/j.dark.2023.101259](https://doi.org/10.1016/j.dark.2023.101259)
- Del Popolo, A., Pace, F., & Le Delliou, M. 2017, J. Cosmol. Astropart. Phys., 2017, 032, doi: [10.1088/1475-7516/2017/03/032](https://doi.org/10.1088/1475-7516/2017/03/032)
- Delos, M. S., Bruff, M., & Erickcek, A. L. 2019, Phys. Rev. D, 100, 023523, doi: [10.1103/PhysRevD.100.023523](https://doi.org/10.1103/PhysRevD.100.023523)
- Delos, M. S., Erickcek, A. L., Bailey, A. P., & Alvarez, M. A. 2018, Phys. Rev. D, 98, 063527, doi: [10.1103/PhysRevD.98.063527](https://doi.org/10.1103/PhysRevD.98.063527)
- Delos, M. S., & Franciolini, G. 2023, Phys. Rev. D, 107, 083505, doi: [10.1103/PhysRevD.107.083505](https://doi.org/10.1103/PhysRevD.107.083505)
- Delos, M. S., & Silk, J. 2023, MNRAS, 520, 4370, doi: [10.1093/mnras/stad356](https://doi.org/10.1093/mnras/stad356)
- Delos, M. S., & White, S. D. M. 2023, MNRAS, 518, 3509, doi: [10.1093/mnras/stac3373](https://doi.org/10.1093/mnras/stac3373)
- Dokuchaev, V. I., & Eroshenko, Y. N. 2002, Sov. J. Exp. Theor. Phys., 94, 1, doi: [10.1134/1.1448602](https://doi.org/10.1134/1.1448602)
- Drakos, N. E., Taylor, J. E., Berrouet, A., Robotham, A. S. G., & Power, C. 2019, MNRAS, 487, 1008, doi: [10.1093/mnras/stz1307](https://doi.org/10.1093/mnras/stz1307)
- Dror, J. A., Ramani, H., Trickle, T., & Zurek, K. M. 2019, Phys. Rev. D, 100, 023003, doi: [10.1103/PhysRevD.100.023003](https://doi.org/10.1103/PhysRevD.100.023003)
- Fakhry, S. 2023, arXiv e-prints, arXiv:2308.11049, doi: [10.48550/arXiv.2308.11049](https://doi.org/10.48550/arXiv.2308.11049)
- Fakhry, S., & Del Popolo, A. 2023, Phys. Rev. D, 107, 063507, doi: [10.1103/PhysRevD.107.063507](https://doi.org/10.1103/PhysRevD.107.063507)
- Fakhry, S., Firouzjaee, J. T., & Farhoudi, M. 2021, Phys. Rev. D, 103, 123014, doi: [10.1103/PhysRevD.103.123014](https://doi.org/10.1103/PhysRevD.103.123014)
- Fakhry, S., Naseri, M., Firouzjaee, J. T., & Farhoudi, M. 2022a, Phys. Rev. D, 105, 043525, doi: [10.1103/PhysRevD.105.043525](https://doi.org/10.1103/PhysRevD.105.043525)
- Fakhry, S., Salehnia, Z., Shirmohammadi, A., & Firouzjaee, J. T. 2022b, APJ, 941, 36, doi: [10.3847/1538-4357/aca523](https://doi.org/10.3847/1538-4357/aca523)
- Fakhry, S., Salehnia, Z., Shirmohammadi, A., Yengejeh, M. G., & Firouzjaee, J. T. 2023a, APJ, 947, 46, doi: [10.3847/1538-4357/acc1dd](https://doi.org/10.3847/1538-4357/acc1dd)
- Fakhry, S., Tabasi, S. S., & Firouzjaee, J. T. 2023b, Phys. Dark Universe, 41, 101244, doi: [10.1016/j.dark.2023.101244](https://doi.org/10.1016/j.dark.2023.101244)
- Franciolini, G., Musco, I., Pani, P., & Urbano, A. 2022, Phys. Rev. D, 106, 123526, doi: [10.1103/PhysRevD.106.123526](https://doi.org/10.1103/PhysRevD.106.123526)
- Franciolini, G., & Urbano, A. 2022, Phys. Rev. D, 106, 123519, doi: [10.1103/PhysRevD.106.123519](https://doi.org/10.1103/PhysRevD.106.123519)
- Gosenca, M., Adamek, J., Byrnes, C. T., & Hotchkiss, S. 2017, Phys. Rev. D, 96, 123519, doi: [10.1103/PhysRevD.96.123519](https://doi.org/10.1103/PhysRevD.96.123519)
- Green, A. M., & Kavanagh, B. J. 2021, J. Phys. G Nucl. Part. Phys., 48, 043001, doi: [10.1088/1361-6471/abc534](https://doi.org/10.1088/1361-6471/abc534)
- Green, A. M., Liddle, A. R., Malik, K. A., & Sasaki, M. 2004, Phys. Rev. D, 70, 041502, doi: [10.1103/PhysRevD.70.041502](https://doi.org/10.1103/PhysRevD.70.041502)
- Griest, K., Cieplak, A. M., & Lehner, M. J. 2014, APJ, 786, 158, doi: [10.1088/0004-637X/786/2/158](https://doi.org/10.1088/0004-637X/786/2/158)
- Hall, A., Gow, A. D., & Byrnes, C. T. 2020, Phys. Rev. D, 102, 123524, doi: [10.1103/PhysRevD.102.123524](https://doi.org/10.1103/PhysRevD.102.123524)
- Hu, W., & Sugiyama, N. 1996, APJ, 471, 542, doi: [10.1086/177989](https://doi.org/10.1086/177989)
- Hütsi, G., Raidal, M., Vaskonen, V., & Veermäe, H. 2021, J. Cosmol. Astropart. Phys., 2021, 068, doi: [10.1088/1475-7516/2021/03/068](https://doi.org/10.1088/1475-7516/2021/03/068)

- Inman, D., & Ali-Haïmoud, Y. 2019, *Phys. Rev. D*, 100, 083528, doi: [10.1103/PhysRevD.100.083528](https://doi.org/10.1103/PhysRevD.100.083528)
- Jung, S., & Shin, C. S. 2019, *Phys. Rev. Lett.*, 122, 041103, doi: [10.1103/PhysRevLett.122.041103](https://doi.org/10.1103/PhysRevLett.122.041103)
- Karam, A., Koivunen, N., Tomberg, E., Vaskonen, V., & Veermäe, H. 2023, *J. Cosmol. Astropart. Phys.*, 2023, 013, doi: [10.1088/1475-7516/2023/03/013](https://doi.org/10.1088/1475-7516/2023/03/013)
- Kohri, K., Nakama, T., & Suyama, T. 2014, *Phys. Rev. D*, 90, 083514, doi: [10.1103/PhysRevD.90.083514](https://doi.org/10.1103/PhysRevD.90.083514)
- Kolb, E. W., & Tkachev, I. I. 1994, *Phys. Rev. D*, 50, 769, doi: [10.1103/PhysRevD.50.769](https://doi.org/10.1103/PhysRevD.50.769)
- Korwar, M., & Profumo, S. 2023, *J. Cosmol. Astropart. Phys.*, 2023, 054, doi: [10.1088/1475-7516/2023/05/054](https://doi.org/10.1088/1475-7516/2023/05/054)
- Lacey, C., & Cole, S. 1994, *MNRAS*, 271, 676, doi: [10.1093/mnras/271.3.676](https://doi.org/10.1093/mnras/271.3.676)
- Martinelli, M., Scarcella, F., Hogg, N. B., et al. 2022, *J. Cosmol. Astropart. Phys.*, 2022, 006, doi: [10.1088/1475-7516/2022/08/006](https://doi.org/10.1088/1475-7516/2022/08/006)
- Nakama, T., Kohri, K., & Silk, J. 2019, *Phys. Rev. D*, 99, 123530, doi: [10.1103/PhysRevD.99.123530](https://doi.org/10.1103/PhysRevD.99.123530)
- Niikura, H., Takada, M., Yokoyama, S., Sumi, T., & Masaki, S. 2019, *PhRvD*, 99, 083503, doi: [10.1103/PhysRevD.99.083503](https://doi.org/10.1103/PhysRevD.99.083503)
- Planck Collaboration, Aghanim, N., Akrami, Y., et al. 2020, *AAP*, 641, A6, doi: [10.1051/0004-6361/201833910](https://doi.org/10.1051/0004-6361/201833910)
- Press, W. H., & Schechter, P. 1974, *APJ*, 187, 425, doi: [10.1086/152650](https://doi.org/10.1086/152650)
- Reed, D., Gardner, J., Quinn, T., et al. 2003, *MNRAS*, 346, 565, doi: [10.1046/j.1365-2966.2003.07113.x](https://doi.org/10.1046/j.1365-2966.2003.07113.x)
- Reed, D., Governato, F., Verde, L., et al. 2005, *MNRAS*, 357, 82, doi: [10.1111/j.1365-2966.2005.08612.x](https://doi.org/10.1111/j.1365-2966.2005.08612.x)
- Ricotti, M., & Gould, A. 2009, *APJ*, 707, 979, doi: [10.1088/0004-637X/707/2/979](https://doi.org/10.1088/0004-637X/707/2/979)
- Sabti, N., Muñoz, J. B., & Blas, D. 2022, *ApJL*, 928, L20, doi: [10.3847/2041-8213/ac5e9c](https://doi.org/10.3847/2041-8213/ac5e9c)
- Sasaki, M., Suyama, T., Tanaka, T., & Yokoyama, S. 2016, *Phys. Rev. Lett.*, 117, 061101, doi: [10.1103/PhysRevLett.117.061101](https://doi.org/10.1103/PhysRevLett.117.061101)
- . 2018, *Class. Quantum Gravity*, 35, 063001, doi: [10.1088/1361-6382/aaa7b4](https://doi.org/10.1088/1361-6382/aaa7b4)
- Sheth, R. K. 1998, *MNRAS*, 300, 1057, doi: [10.1046/j.1365-8711.1998.01976.x](https://doi.org/10.1046/j.1365-8711.1998.01976.x)
- Sheth, R. K., Mo, H. J., & Tormen, G. 2001, *MNRAS*, 323, 1, doi: [10.1046/j.1365-8711.2001.04006.x](https://doi.org/10.1046/j.1365-8711.2001.04006.x)
- Sheth, R. K., & Tormen, G. 2002, *MNRAS*, 329, 61, doi: [10.1046/j.1365-8711.2002.04950.x](https://doi.org/10.1046/j.1365-8711.2002.04950.x)
- Silk, J. 2000, *Astrophys. Lett. Commun.*, 37, 315
- Stücker, J., Ogiya, G., Angulo, R. E., Aguirre-Santaella, A., & Sánchez-Conde, M. A. 2023, *MNRAS*, 521, 4432, doi: [10.1093/mnras/stad844](https://doi.org/10.1093/mnras/stad844)
- Tinker, J., Kravtsov, A. V., Klypin, A., et al. 2008, *APJ*, 688, 709, doi: [10.1086/591439](https://doi.org/10.1086/591439)
- Tisserand, P., Le Guillou, L., Afonso, C., et al. 2007, *AAP*, 469, 387, doi: [10.1051/0004-6361:20066017](https://doi.org/10.1051/0004-6361:20066017)
- Tokeshi, K., Inomata, K., & Yokoyama, J. 2020, *JCAP*, 2020, 038, doi: [10.1088/1475-7516/2020/12/038](https://doi.org/10.1088/1475-7516/2020/12/038)
- Villanueva-Domingo, P., Mena, O., & Palomares-Ruiz, S. 2021, *Front. Astron. Space Sci.*, 8, 87, doi: [10.3389/fspas.2021.681084](https://doi.org/10.3389/fspas.2021.681084)
- Wang, J.-S., Herrera-Martín, A., & Hu, Y.-M. 2021, *Phys. Rev. D*, 104, 083515, doi: [10.1103/PhysRevD.104.083515](https://doi.org/10.1103/PhysRevD.104.083515)
- Warren, M. S., Abazajian, K., Holz, D. E., & Teodoro, L. 2006, *APJ*, 646, 881, doi: [10.1086/504962](https://doi.org/10.1086/504962)
- White, S. D. M. 2022, *MNRAS*, 517, L46, doi: [10.1093/mnrasl/slac107](https://doi.org/10.1093/mnrasl/slac107)
- Zentner, A. R. 2007, *Int. J. Mod. Phys. D*, 16, 763, doi: [10.1142/S0218271807010511](https://doi.org/10.1142/S0218271807010511)